Comparison of fatigue performance of HVOF spray coated and conventional roll bonded aluminium bearing alloys

M. S. Ali*, P. A. S. Reed and S. Syngellakis

A comparative study on fatigue resistance of thin aluminium bearing linings (supported by harder backing steel layers) produced by high velocity oxyfuel (HVOF) spray coating and conventional roll bonding (RB) processes has shown that the former is superior to the latter with similar lining composition (Al–20%Sn–1%Cu–0?25%Mn) when compared on the basis of oscillating lining surface strains under a three point bend test condition. In terms of the integrity of the multilayered bearing system under oscillating stresses, HVOF lining appeared to show worse fatigue resistance, due to poor/brittle bond between the lining and the backing steel layer resulting in the detachment of the lining from the backing layer. The newly developed RB alloy with reduced Sn content (Al–6?5Sn–2?5Si–1Ni–1Cu–0?25Mn) and scattered intermetallics showed higher fatigue resistance than the HVOF and previous RB systems. This was linked to delayed initiation of short cracks leading to a longer overall lifetime compared to all other systems.

Keywords: Plain bearings, Roll bonding (RB), High velocity oxyfuel (HVOF), Fatigue life, Crack initiation, Short crack

Introduction

Multilayered plain bearing systems are used as connecting rod big end and crank shaft main bearings. The lining layer in modern designs of such systems is a multiphase Al alloy comprising soft Sn, with or without hard Si particles, sometimes including elements such as Ni, Cu and Mn which form intermetallics. The engine loads when transferred to the bearing lining via a thin oil film give rise to hydrodynamic pressure concentrations at various locations of the bearing lining that may initiate fatigue damage at a microscale level initially, leading to lining spalling and seizure. Research at Southampton has extensively focused upon understanding microstructural fatigue initiation and growth in various Al based multiphase lining alloys (in the form of thin layers , 20–30 mm) as well as crack penetration through subsurface layers of widely varying mechanical properties. Earlier work[1] on roll bonding (RB) systems such as AS16 (Al–20Sn–1Cu–0?25Mn) and AS1241 (Al–12Sn–4Si–1Cu) concluded that the size, shape and distribution of secondary phase particles in the lining material have a significant effect upon the initiation and growth of fatigue cracks with fatigue crack initiation occurring via decohesion of these second phase particles from the surrounding matrix. In multilayered bearings, it was found that the layered material structure has a considerable influence on the mesoscopic growth of fatigue cracks.[2] The present paper addresses the mechanism of fatigue failure in various newly developed systems with Al alloy lining layers of different compositions manufactured via RB and high velocity oxyfuel (HVOF) spray coating processes. Such systems are expected to have greatly reduced distributions of Si and Sn particles which have acted as initiation sites in previously reported work.[1]

Materials Research Group, School of Engineering Sciences, University of Southampton, Highfield Southampton, SO17 1BJ, UK

*Corresponding author, email ssarfraz_a@hotmail.com

Materials and experimental techniques

The materials provided by the bearings manufacturers were in the form of trilayer flat bars formed by a series of rolling and intermediate heat treatments as well as finished bearings obtained through final cold forming of these flat bars. The bilayer HVOF spray coated flat bars were produced by Nottingham University. A brief summary of all these systems with their labels, layer types, compositions and relative thicknesses is given in 1. Optical and scanning electron microscopy was used for microstructural analysis. To assess mechanical properties (to be used in subsequent modelling), standard dog bone specimens obtained from individual layers of RB systems (provided as monolithic lining, inter- and steel layers) were subjected to a tensile test at displacement rate of 5 mm min^{21} using an Instron electromechanical tensile testing machine according to British standards.[3] To estimate the effects of work hardening caused by final bearing forming, microhardness tests were also performed on the individual layers in each system as well as the original monolithic layers using a Matsuzava microhardness indenter.

Fatigue tests were conducted using an Instron servohydraulic fatigue testing machine at a load ratio

Published by Maney on behalf of the Institute
Received 8 April 2008; accepted 6 May 2008
DOI 10.1179/174328408X322213

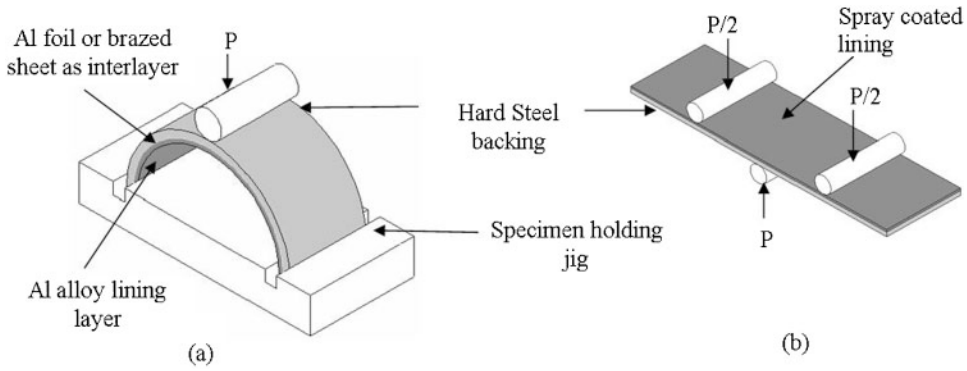

1 Schematic of three point bend fatigue test of a RB bearing b spray coated flat bar

of 0?1 and frequency of 10 Hz using a three point bend test configuration (Fig. 1). Maximum strain developed at the lining surface of a bearing and a flat bar was estimated through elastoplastic finite element model.[4] These numerical results were validated and modified to account properly for the actual support conditions through systematic strain gauge measurements. Bearing specimens were subjected to uninterrupted fatigue lifetime tests whereas the lining surface of flat bar specimens was monitored via acetate replication by interrupting the fatigue test at frequent intervals to observe short crack initiation and growth behaviour.

Results and analysis

Microstructural characteristics of different layers

Figure 2a is an optical micrograph of a cross-section of the AS20S bearing system showing the microstructure and the layered architecture. An SEM image representative of the lining layer microstructure of both the AS20S and AS20 systems is also shown in Fig. 2c. The sole difference between these systems is the presence of a microstructurally complex brazed sheet as an interlayer in the AS20 system instead of a pure Al foil as in the AS20S system. The layered architecture of the HVOF spray coated bimetal flat bar system is shown in Fig. 2b along with an SEM image of the lining layer in Fig. 2d. The lining layer of the AS20S/AS20 system consists of numerous intermetallics and very few Si particles all encapsulated within the Sn phase. Sn films surrounding the harder Si and intermetallic particles are the result of recrystallisation of the Al grains during intermediate heat treatment processes (during roll bonding) as Sn is mostly liquid at these temperatures.[5] Using a finite body tessellation image analysis technique,[6] the average particle area of Sn, Si and intermetallics was found to be 27?55 ¡ 21?85, 14?7 ¡ 14?21 and 28?05 ¡ 16?64 mm^2 respectively. Compared to the previously developed AS16 system,[1] the AS20S lining surface showed much finer Sn particles with widely scattered intermetallics and in comparison to the AS1241 system, fewer and more widely scattered Si particles were observed.

The cross-section of the monolithic brazed sheet used as interlayer in the AS20 (Fig. 2e) showed the presence of a large number of Si particles in the narrow strip (, 50 mm in thickness) of 4343 layer and widely scattered Al–Mn type intermetallics (analysed through EDX) in the 3003 layer (, 120 mm in thickness). Actual brazed sheet within the finished bearing was too thin (40 mm) and was therefore hard to resolve in the form of two layers under optical and scanning electron microscopes.

In comparison with the RB systems, the microstructure of the HVOF lining surface is more complex and less clear under optical microscopy. The circular features appear to be unmelts resulting from inefficient melting and high speed deposition of the original powder particles. The backscattered electron imaging (BEI) image of the lining surface is shown in Fig. 2d which clearly indicates the Sn phase (white areas), Al matrix (dark) and intermetallic particles (light grey areas). The BEI image hints at a very fine and scattered distribution of Sn but more clearly shows the larger smeared out white Sn regions between splats. Previous TEM work[7] has indicated that the expected distribution of Sn within the HVOF coating is very fine on the scale of nanometres. However a heterogeneous distribution of Sn at the scale of splats/unmelts is likely to arise due to squeezing out of molten Sn between these features during the spray coating process.

Table 1 Material system specifications: medium carbon steel backing of between 1?8 and 1?9 mm thickness, brazed sheet is combination of 3003 alloy* (Al–1?2Mn–0?6Cu–0?7Fe) and 4343 alloy{ (Al–6Si–0?8Fe–0?25Cu)

Material system		Lining layer		Interlayer		Specimen dimensions, mm
Bearings	Name	Composition, wt-%	Thickness, mm	Composition, wt-%	Thickness, mm	Radius6width or length6width
Bearing	AS20S	Al–6–8Sn–2·5Si–1Cu–1Ni–0·25Mn	0·30–0·40	Al	0·04	296 28
	AS20	Al–6–8Sn–2·5Si–1Cu–1Ni–0·25Mn	0·30–0·40	3003*	0·038	296 28
				4343{	0·002	
Flat bar	AS20S	Al–6–8Sn–2·5Si–1Cu–1Ni–0·25Mn	0·18–0·30	Al	0·04	796 19·5
	AS20	Al–6–8Sn–2·5Si–1Cu–1Ni–0·25Mn	0·18–0·30	3003*	0·038	796 19·5
				4343{	0·002	
	HVOF	Al–20Sn–1Cu	0·18–0·40	None		596 25

*Al–1?2Mn–0?6Si–0?7Fe.
{Al–6Si.

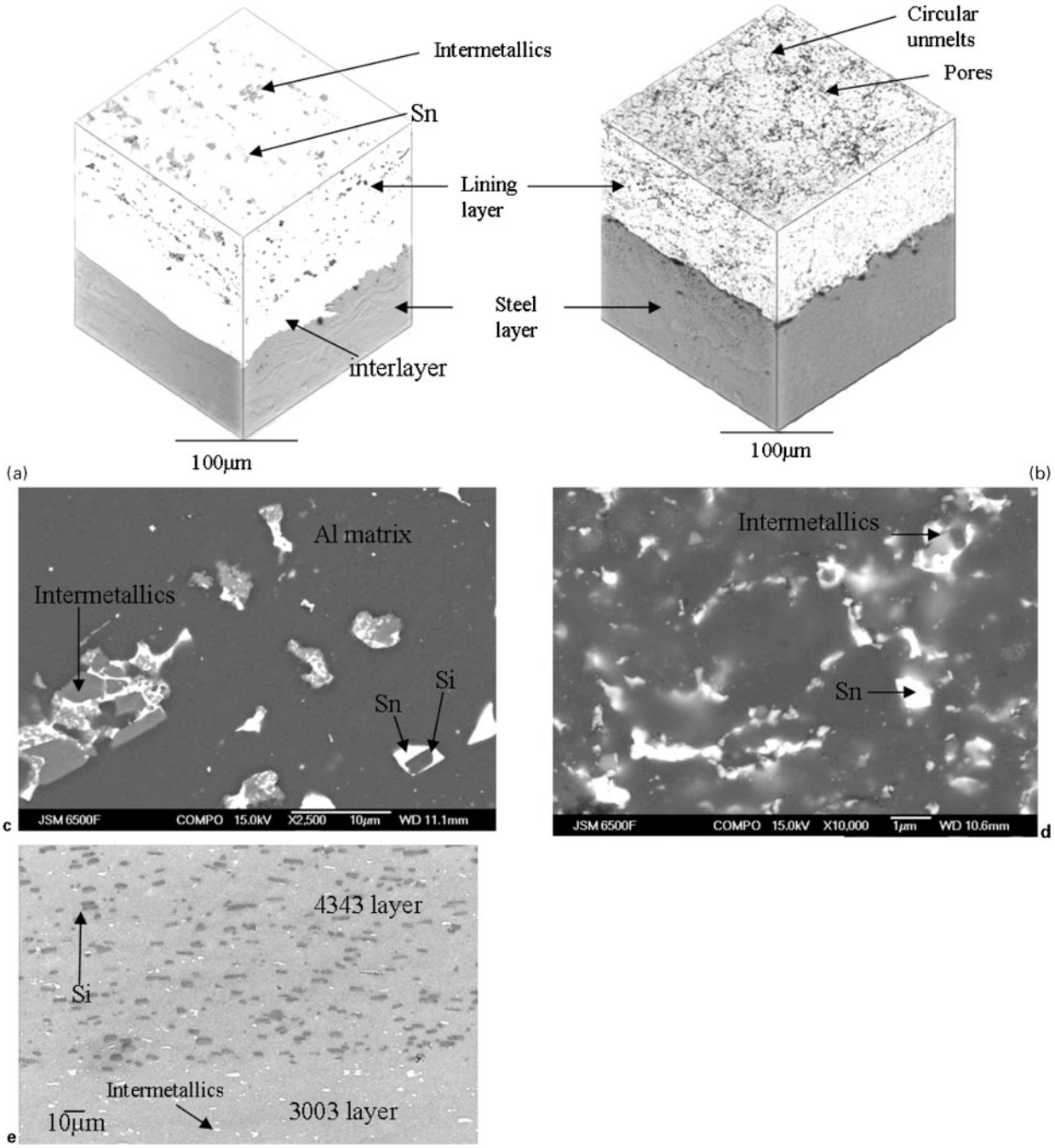

2 Optical images of cross-sections of a AS20S and b HVOF flat bar system, SEM images of c AS20S and d HVOF lining surfaces, e monolithic brazed sheet used as interlayer for AS20SFS system

Mechanical properties of different layers

Figure 3 shows the tensile properties of the monolithic layers in each new system compared with previous data on AS16 and AS1241. The monolithic lining and interlayers of the AS20S/AS20 system are those obtained before to the roll bonding process; however there was no HVOF monolithic layer available and hence true tensile test data for the HVOF lining could not be obtained. As microhardness values of the HVOF lining surface were found to be closer to the AS20S lining (shown in Table 2), hence tensile test data obtained for the AS20S monolithic lining were used for the finite element (FE) modelling of the HVOF flat bars. Microhardness tests showed that the AS20S lining layers in general were harder (HV557 ¡ 8) than the spray coated lining (HV553 ¡ 7). Furthermore the AS20S lining showed higher yield stress and ultimate tensile strength (UTS) when compared with the lining layers of the previously manufactured AS1241 system.

The steel layers of all new and old RB systems showed higher yield strength and UTS compared to the HVOF steel layer which was essentially low carbon steel and was heat treated after manufacture and received very little or no cold work. Vickers microhardness number values obtained for monolithic, flat bar and bearing lining layers did not show much difference (, 5% for

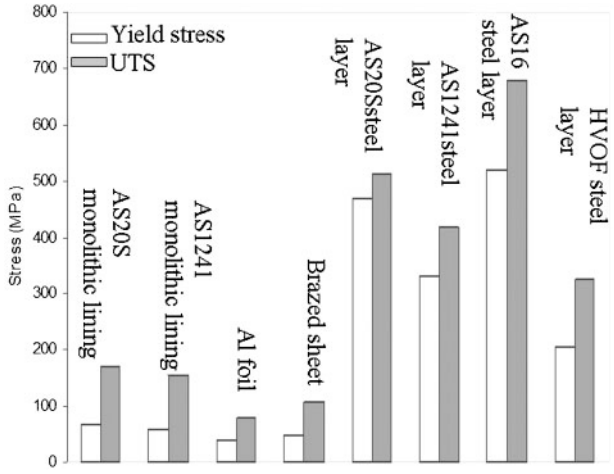

3 Tensile test results for different monolithic layers

AS20S/AS20 systems) and hence the presence of any residual stresses in the finished bearings could be ignored in subsequent FE modelling.

Fatigue test results

Fatigue lifetime results are based upon maximum plastic strain e_p developing at the lining surface during a three point bend test v. number of cycles to fail the specimen. The values of e_p have been estimated by an existing two-dimensional elastoplastic FE model[4] using true s logarithmic e data derived from the tensile test data performed on the available monolithic layers of the systems studied. As mentioned earlier, the FE simulated e_p was compared with respective experimental measurements; as a result, a correction factor was applied to the calculated e_p and used in the subsequent fatigue lifetime data.

Fatigue lifetime data were obtained from a number of uninterrupted fatigue tests performed on finished bearings whereas interrupted fatigue tests with periodic acetate replication were conducted upon flat bar specimens for short crack initiation and growth analysis. Fatigue behaviour of all these systems in terms of total lifetime and short crack growth was observed to vary with systems of different lining layer compositions.

Table 2 Microhardness test results for various layers

Material systems	Lining layer	Interlayer	Backing layer
AS20S/AS20 bearing	57 ¡ 8	39 ¡ 3/47 ¡ 2	187 ¡ 3
AS20S/AS20 monolithic	54 ¡ 9	38 ¡ 2/43 ¡ 3	NA
AS1241 bearing	54 ¡ 6	36 ¡ 7	168 ¡ 11
AS1241 monolithic	41 ¡ 4	NA	NA
AS16 bearing	45 ¡ 3	34 ¡ 4	190 ¡ 23
HVOF flat bar	53 ¡ 4	NA	112·5

Fatigue lifetime results

The fatigue lifetime v. de_p (maximum plastic strain range) for different RB systems for both bearing and flat bar specimens is shown in Fig. 4 and compared with the fatigue lifetime result for the HVOF flat bar specimens. The overall fatigue lifetime trend for all RB systems is independent of the specimen geometry as both bearing and flat bar specimens showed similar fatigue lifetime results within the expected experimental scatter. It is evident that the newly developed AS20S/AS20 systems showed better fatigue resistance than the previous RB systems with the HVOF flat bar results being broadly comparable to the AS20S/AS20 systems. There was no significant difference in the observed total fatigue lifetime of the AS20S and AS20 finished bearing systems.

Microscale surface fatigue damage

The observed differences in the total fatigue lifetime can be linked to differences in the initiation and growth of short fatigue cracks at the lining surface where maximum e_p develops during fatigue testing. The actual bearing surface is curved and it was difficult to replicate it during interrupted fatigue tests to capture the growth of short fatigue cracks. However similar lifetime trends

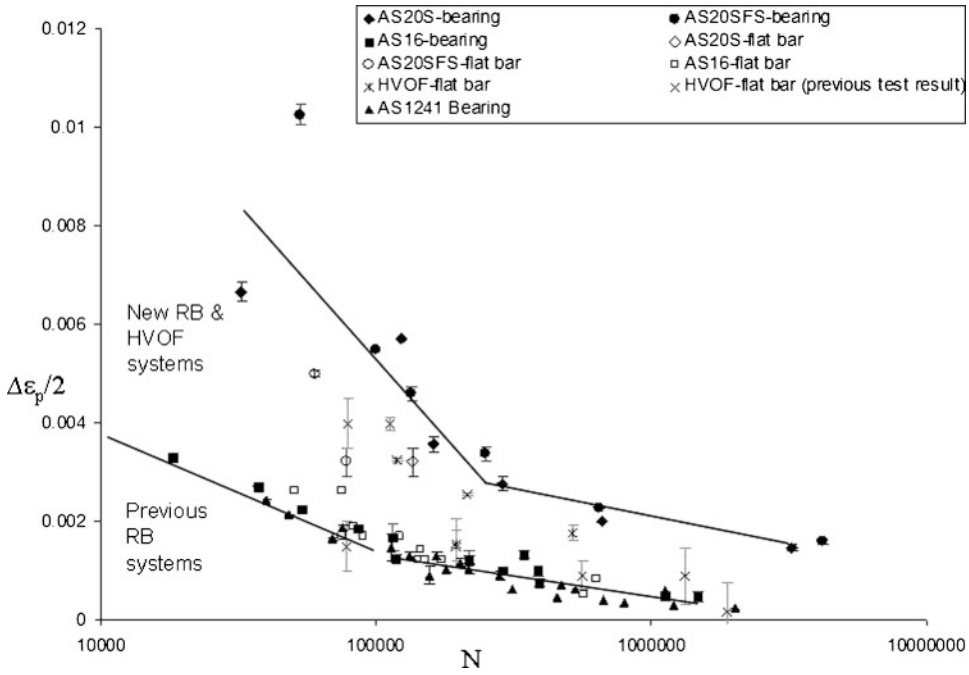

4 Fatigue lifetime data from previous[1] and current work strain lifetime data

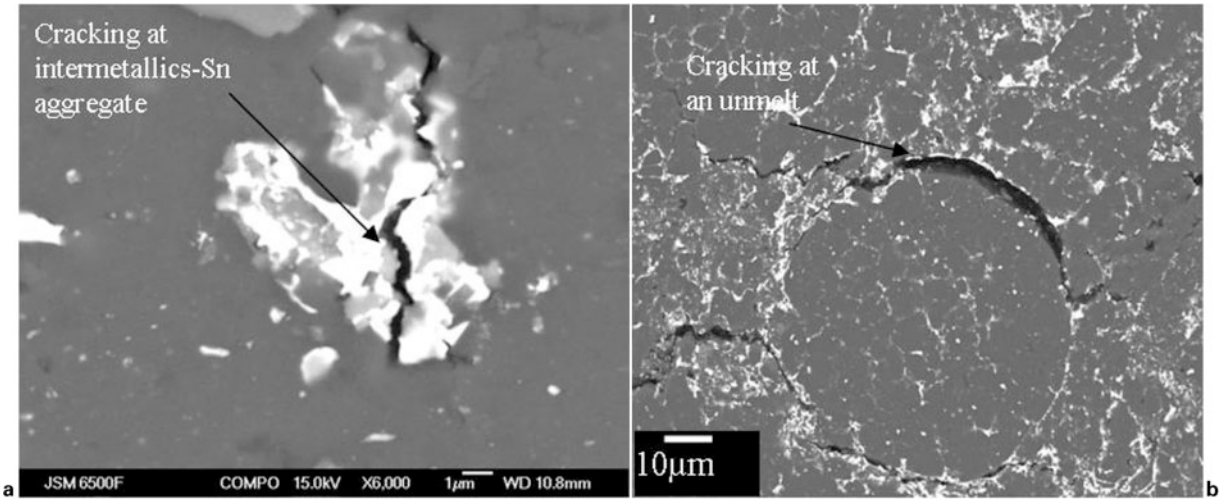

5 Backscattered electron image showing short crack initiating from a AS20S and b HVOF lining surface

observed for both bearing and flat bar specimens gave confidence in using flat bar specimen surface to analyse the microscale fatigue damage and link these observations to actual fatigue initiation in the bearing specimens.

Results from the RB and HVOF flat bars tested at similar e_p (0?0054) showed that, for the AS20S/AS20 lining, cracks appeared to be initiating from widely scattered intermetallics encapsulated within thin layers (, 2–6 mm) of Sn as shown in Fig. 5a. Far fewer initiation sites were observed in comparison with the AS1241 and AS16. Cracking of individual intermetallics was also observed with very few individual Sn particles showing initiation. These cracks grew steadily until shielding effects from the harder backing layer slowed growth as their subsurface length approached the lining thickness (0?15–0?30 mm) towards the end of life.

In the case of HVOF lining, the crack initiating sites are circular unmelts left during the spray coating process as shown in Fig. 5b although some cracks also appeared to be initiating from widely distributed pores and growing towards Sn rich areas. The average size of the initiating unmelts was found to be 15–20 mm and the cracks initiated grew very quickly (to , 0?3–1 mm) within a fraction of total lifetime (N/N_f) as small as 0?5%. After this rapid initial stage, the cracks grew steadily and then their growth slowed down due to the shielding effects of the backing layer. A comparison of the crack growth behaviour of the various linings can be made by referring to Fig. 6 showing da/dN v. projected crack length in mm.

Post fatigue failure analysis

Failed RB bearings and HVOF flat bar specimens were sectioned and polished to observe subsurface crack trajectories through the multilayered structure. Cracks in the AS20S system appeared to deflect within the softer Al layer (Fig. 7a). Similar crack trajectories have been observed in previously tested AS1241 and AS16 systems[1,4] and the phenomenon was linked to the sudden decrease in the crack tip driving force as the crack crosses the lining/interlayer interface due to the presence of the harder steel backing. The crack in the case of the AS20 system appeared to be penetrating deeply into the brazed sheet (Fig. 7b). This was unexpected since the stress profile across different layers evaluated on the basis of the elastoplastic FE model did not show any differences between the two systems. However, further study of the failed specimens via SEM indicated that the crack had actually deflected within the softer 4343 layer (a very thin part of the brazed sheet with HV 45 contrary to the 3003 with HV 49) which is adjacent to the harder steel backing layer. In the case of the HVOF system, the crack appeared to debond the lining layer completely from the backing layer (Fig. 7c).

Discussion

The newly developed AS20S/AS20 bearing systems have been manufactured essentially using the same rolling techniques as used for the old systems; however their lining layer contained much less Sn (compared to the AS16 lining) and Si (compared to the AS1241 lining) particles with respectively a larger amount of a widely scattered and relatively large intermetallics. Energy dispersive X-ray analysis showed that these intermetallics were mostly of $AlNi_4$ type which is known to be harder than the matrix and Sn particles. Some evidences of $CuAl_2$ type intermetallics were also found. The role of Cu and Ni is to improve the strength of the alloy (by solid solution strengthening) and to form intermetallics of the type $CuAl_2$, $AlNi_4$ and AlNi.[8,9] The elevated hardness, yield strength and UTS of the AS20S lining

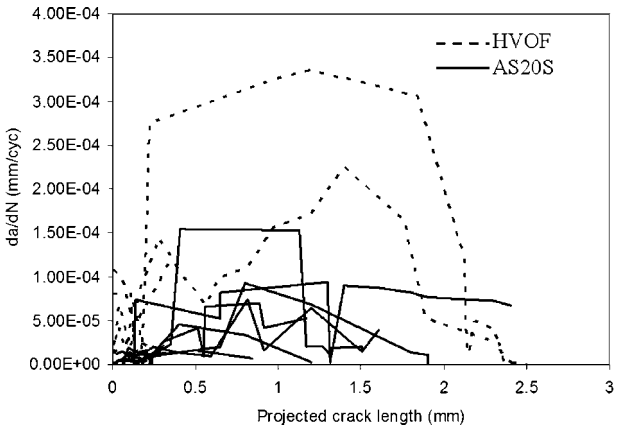

6 Lining surface short fatigue crack growth rate v. crack length for RB and HVOF systems

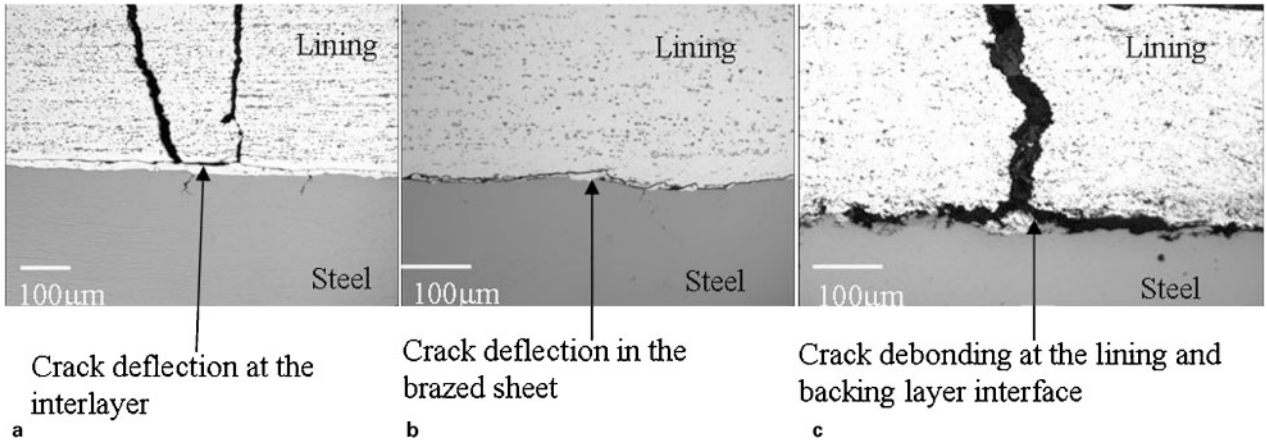

7 Optical images showing subsurface deflection of fatigue cracks in a AS20S, b AS20 and c HVOF system

compared to the previous AS1241 lining re the result of these compositional modifications.

Fatigue failure started at the lining surface where maximum e_p develops. Nanoindentation on the intermetallic particles (reported in detail elsewhere)[10] confirmed that they were harder than the matrix and the Sn phase. Softer Sn particles (E5 41 GPa) are more compliant than comparatively harder intermetallics (E5 100–200 GPa). Also the morphology of the microstructure (clusters of both Sn and intermetallics) is quite irregular. Sn films surrounding the intermetallics result in a significant compliance mismatch that might have led to high stress concentrations causing crack initiation by detaching softer Sn films from harder intermetallics. At similar plastic strain levels, initiation in the HVOF lining was observed extremely early in the fatigue lifetime (N/N_f , 0?5%) with multiple crack initiation sites. These cracks appeared to be originating mostly from the interface between the unmelts and the Al matrix. As Sn particles are found to be of much finer size within the splats (compared to the Sn particles in all RB systems), these fine Sn dispersions were not seen to be associated with initiation. However relatively larger Sn rich regions around the unmelt peripheries seemed to contribute to initiation. The difference in the compliance between Sn rich (at nanoscale size level) Al matrix and circular unmelts surrounded by relatively coarser Sn regions may cause initiation. This could also be linked to weaker interface between unmelt and the surrounding. There is also a possibility that the oxide layer/oxide particle formation around particles during spraying are the likely sites of crack initiation during subsequent fatigue of the HVOF lining.

When the dominant crack reached an appreciable subsurface depth, it deflected within the interlayer at 90u to the normal growth mode. Suresh et al.[11] proposed that the local compliance ahead of a crack increases as it approaches the interface from a softer side and reduces in the opposite case. The increase in the compliance was considered to inhibit the continued growth of the crack in mode I direction causing it to deflect. The deflection of the crack within the soft Al interlayer in the AS20S bearing is in agreement with previous work by Joyce[4] according to which the fatigue crack penetrates from a harder lining into the softer Al interlayer due to antishielding and then deflects in the interlayer due to the shielding effect of the harder backing layer. The AS20 system has a more complex interlayer structure, which is expected to be harder than the pure Al foil in most of the RB systems. It was thought that this might restrict subsurface growth of the crack by promoting early deflection and hence increase fatigue life, however the AS20S and AS20 systems did not show appreciable differences in observed lifetime. Within the brazed sheet, the 4343 layer (adjacent to the steel layer) was found to be softer than the 3003 layer from micro- and nanohardness results. As the subsurface crack tip approaches the 3003 layer there is an increase in the crack tip driving force as the 3003 layer is softer than the AS20 lining. This driving force further increases when the crack tip interacts with the even softer 4343 layer, but once the crack tip enters the softest 4343 layer it is expected to experience shielding and deflect within the 4343 layer due to the influence of the steel backing. Since the thickness of the 4343 layer was , 10% of the whole brazed sheet (i.e. 4 mm) post failure analysis to confirm this interpretation is quite challenging.

Although the early growth of cracks on the HVOF surface was fast (mostly originating from interface of the circular unmelts and the matrix), the later growth was extremely sluggish giving HVOF a comparable lifetime to that of RB systems. However investigation of the failed specimen showed a complete failure at the steel/lining interface indicating a poor interfacial strength in the present system. Hence the applied load during fatigue test may not have transferred completely to the lining surface that resulted in the sluggish growth of cracks after instant initiation and fast growth. This has resulted in the HVOF lining appearing comparable to the RB systems in overall fatigue lifetime predictions; however there are critical issues of considerable lining detachment from the backing layer and hence the simple laboratory lifetime estimations in terms of e_p range and observations of surface crack growth behaviour are not a guarantee of the comparable performance of the HVOF bearing during actual engine operation. The integrity of the bonds between the lining layer, interlayer and backing layers of the RB systems keeps them essentially intact even after the subsurface penetration of the cracks. Significant detachment of portions of the HVOF lining in service will result in seizure of the bearings.

Conclusion

The microstructure of the AS20S/AS20 lining with much fewer and finer Sn and Si particles showed improved resistance to the initiation of short fatigue cracks which

resulted in delayed fatigue damage (via decohesion of Sn and intermetallics) and hence much better fatigue lifetime compared to that of the previously studied RB systems. The harder brazed sheet used as an interlayer in the basic AS20 system did not retard subsurface penetration of cracks and hence the observed lifetime of the AS20S system was not significantly different from that of the AS20 system. In the HVOF system crack deflection along the apparently weak interface resulted in the debonding of the lining layer that could cause spalling off the lining during service. Hence the HVOF, although showing similar lifetime behaviour in these tests, could not be considered comparable in overall performance to the RB systems in the bearing application.

Acknowledgement

Dana Glacier Vandervell bearings (UK), University of Southampton and University of Nottingham are gratefully acknowledged for providing materials and helpful discussions.

References

1. M. C. Mawanza, M. R. Joyce, K. K. Lee, S. Syngellakis and P. A. S Reed: Int. J. Fatigue, 2003, 25, 1135–1145.
2. M. R. Joyce, P. A. S Reed and S. Syngellakis: Mater. Sci. Eng. A, 2003, A342, 11–22.
3. 'Tensile testing of metallic materials – Part 1: method of test at ambient temperature', EN 10002-1, BSI, London, UK, 1990.
4. M. R. Joyce: 'Fatigue of aluminium linings in plain automotive bearings', PhD thesis, University of Southampton, UK, 2000.
5. E. R. Braithwaite: 'Lubrication and lubricants', 355; 1967, Amsterdam, Elsevier Publishing Company.
6. J. Boselli, P. J. Gregson and I. Sinclair: J. Microsc., 1999, 195, 104–112.
7. S. J. Harris, D. G. McCartney, A. J. Horlock and C. Perrin: Mater. Sci. Forum, 2000, 331–337, 519–526.
8. N. L. Tawfik: J. Mater. Sci., 1997, 32, 2997–3000.
9. J. Hogerls, S. Spaic and H. Tensi: Aluminum, 1998, 74, (Jahrgang 10), 780.
10. M. S. Ali, P. A. S. Reed, S. Syngellakis, A. J. Moffat and C. Perrin: Mater. Sci. Forum, 2006, 519, 1071–1076.
11. S. Suresh, Y. Sugimuera and E. K. Tschegg: Scr. Metall. Mater., 1992, 27, 1189–1194.